ANTIMICROBIAL AGENTS AND CHEMOTHERAPY, July 2011, p. 3432–3438 Vol. 55, No. 7
0066-4804/11/$12.00 doi:10.1128/AAC.01803-10

Synergistic Combination of Chitosan Acetate with Nanoparticle Silver as a Topical Antimicrobial: Efficacy against Bacterial Burn Infections▽

Liyi Huang,[1,2,3]† Tianhong Dai,[1,2]† Yi Xuan,[1,4] George P. Tegos,[1,2,5] and Michael R. Hamblin[1,2,6]*

Wellman Center for Photomedicine, Massachusetts General Hospital, Boston, Massachusetts[1]; Department of Dermatology, Harvard Medical School, Boston, Massachusetts[2]; Department of Infectious Diseases, First Affiliated College and Hospital, Guangxi Medical University, Nanning, China[3]; School of Engineering, Tufts University, Medford, Massachusetts[4]; Department of Pathology, University of New Mexico School of Medicine, Albuquerque, New Mexico[5]; and Harvard-MIT Division of Health Sciences and Technology, Cambridge, Massachusetts[6]

Received 22 December 2010/Returned for modification 27 February 2011/Accepted 10 April 2011

Chitosan and nanoparticle silver are both materials with demonstrated antimicrobial properties and have been proposed singly or in combination as constituents of antimicrobial burn dressings. Here, we show that they combine synergistically to inhibit the *in vitro* growth of Gram-positive methicillin-resistant *Staphylococcus aureus* (MRSA) and Gram-negative bacteria (*Pseudomonas aeruginosa*, *Proteus mirabilis*, and *Acinetobacter baumannii*), as judged by bioluminescence monitoring and isobolographic analysis, and also produce synergistic killing after 30 min of incubation, as measured by a CFU assay. The hypothesized explanation involves chitosan-mediated permeabilization of bacterial cells, allowing better penetration of silver ions into the cell. A dressing composed of freeze-dried chitosan acetate incorporating nanoparticle silver was compared with a dressing of chitosan acetate alone in an *in vivo* burn model infected with bioluminescent *P. aeruginosa*. The survival rates of mice treated with silver-chitosan or regular chitosan or left untreated were 64.3% ($P = 0.0082$ versus regular chitosan and $P = 0.0003$ versus the control), 21.4%, and 0%, respectively. Most of the fatalities occurred between 2 and 5 days postinfection. Silver-chitosan dressings effectively controlled the development of systemic sepsis, as shown by blood culture. These data suggest that a dressing combining chitosan acetate with silver leads to improved antimicrobial efficacy against fatal burn infections.

Bacterial infections in serious burns have been a constant threat to human health throughout history. Infections that develop in traumatic and surgical wounds and burns remain a major problem despite decades of advances in antibiotics and antiseptics (38). Many burn infections are treated with antibiotics that can be applied topically or administered orally or by injection. Unfortunately, due to the excessive use of antibiotics, some bacteria have evolved to become antibiotic resistant, and this has led to the present time being described as the "end of the antibiotic era" (26, 34). Thus, the search for novel, more efficient antibacterial burn dressings has been the subject of intense and continuing research efforts (14, 20, 27). In addition, it has recently been recognized that certain bacterial strains, such as *Pseudomonas aeruginosa*, have the ability to establish themselves in biofilms (2, 28, 47), which are complex structures consisting of bacterial cells embedded in an extracellular matrix of hydrated extrapolymeric substances and permanently attached to surfaces (13). Biofilms can act as efficient barriers against antibiotics and the host immune system and subsequently render the bacterial infections persistent and more difficult to eradicate (13). Bacteria living in biofilms can be up to 1,000 times more resistant to antibacterial compounds than their planktonic counterparts (39). As a result of the therapeutic failure of some front-line antibiotics, the medical community is faced with developing new treatment modalities.

The antimicrobial properties of silver have been known from antiquity: the Egyptians, Greeks, Romans, and other ancient civilizations used silver vessels to store perishable foods, and silver cutlery, cups, and dishes were used by the rich (17). While the discovery of penicillin led to the era of synthetic antibiotics, increasing antibiotic resistance of bacteria and the ineffectiveness of synthetic antibiotics against some bacterial strains have led to the reemergence of interest in silver, silver salts, silver compounds, and nanocrystalline silver as antibacterial agents (8, 18, 41).

It is known that chitosan, the N-deacetylated derivative of chitin, has significant antibacterial activity against a broad spectrum of bacteria (43). We have previously investigated the use of a chitosan acetate bandage (the HemCon bandage) for the treatment of infected excisional wounds (5, 6) and burns (15). We studied 10-s full-thickness third-degree burns infected with 10^7 CFU of *Pseudomonas aeruginosa* in a mouse model. It was found that a chitosan acetate bandage significantly increased the survival rate of mice compared with untreated controls (73.3% versus 13.3%; $P < 0.0002$). However, a chitosan acetate bandage was not effective in preventing fatal infections developing from a more severe situation of a 60-s burn infected with 10^8 CFU of *P. aeruginosa* in mice (22.2% survival rate; $n = 9$) (data not shown). We hypothesized that this failure was due to the inability of the chitosan acetate bandage to rapidly eradicate sufficient bacteria in the burn, therefore allowing the surviving *P. aeruginosa* cells to form biofilms in the infected burns. Silver has been reported to be effective in preventing the formation of *P. aeruginosa* biofilms

* Corresponding author. Mailing address: BAR414, Wellman Center for Photomedicine, Massachusetts General Hospital, 40 Blossom Street, Boston, MA 02114. Phone: (617) 726-6182. Fax: (617) 726-8566. E-mail: hamblin@helix.mgh.harvard.edu.

† L.H. and T.D. made equal contributions to this study.

▽ Published ahead of print on 18 April 2011.

TABLE 1. Bacterial strains (bioluminescent) used in the study

Bacterial species or strain	ATCC no.	XEN no.[a]
MRSA US-300		30
A. baumannii	BAA 747	
P. mirabilis	51393	44
P. aeruginosa	19960	5P

[a] The XEN number is the designation from Xenogen Corp. (now Caliper Life Sciences).

and also against fully developed *in vitro* biofilms of *P. aeruginosa* (3, 42).

In recent times, there has been considerable interest in preparations of nanoparticles and films that combine both silver and chitosan (45, 50, 51). Some of these materials have been proposed as wound or burn dressings (33, 49). However, there does not appear to be any report that examines possible synergism between the antibacterial effects of silver and chitosan. In the present study, we investigated the possible synergistic combination of chitosan acetate with nanocrystalline silver for improved antimicrobial efficacy *in vitro* and against burn infections in a mouse model.

MATERIALS AND METHODS

Strains and media. Due to the observation that nanoparticle silver scattered light and was therefore highly turbid, we selected bioluminescent bacteria in this study to facilitate measurement of growth with a plate reader. The turbidity did not affect luminescence measurements because the scattered photons were still measured by the photomultiplier tube. The following microbial strains were used (Table 1): methicillin-resistant *Staphylococcus aureus* (MRSA) (Xen 30), *Proteus mirabilis* ATCC 51393 (Xen 44), and *P. aeruginosa* ATCC 19660 (Xen 5P) (all kind gifts from Xenogen Corp., Alameda, CA), as well as *Acinetobacter baumannii* ATCC BAA 747 (ATCC, Manassas, VA). *A. baumannii* ATCC BAA 747 was transduced with the *luxCDABE* operon (originally cloned from *Photorhabdus luminescens*) as described previously (16). Planktonic bacterial cells were cultured in brain heart infusion (BHI) broth with aeration at 37°C. Cell numbers were estimated by measuring the optical density at 600 nm (OD_{600}) (an OD of 0.5 was equal to 10^8 cells/ml, as confirmed by plate counts).

Materials. The chitosan-lactate gel consisted of 2% chitosan in 2% lactic acid and was prepared by dissolving ultrapure chitosan (Protasan UPB; degree of deacetylation, 91%; molecular weight [MW], 460,000; FMC NovaMatrix, Sandvika, Norway) in lactic acid solution. The nanoparticle silver suspension was a 0.2% (wt/wt) suspension of nanoparticle silver in distilled H_2O and was prepared from Nanohorizons Polyform AS (Nanohorizons, Bellefonte, PA) containing a proprietary stabilizer.

The freeze-dried chitosan acetate dressing (HemCon bandage; HemCon Medical Technologies Inc., Portland, OR) has been previously described (6). The silver-containing chitosan acetate dressing was similar to the nonsilver version with the exception of the inclusion of a uniform dispersion of 400 ppm of nanoparticulate silver (Polyform AS) in the chitosan gel that was used to prepare the freeze-dried dressings.

MIC determinations. The antibacterial activities of chitosan acetate and silver were determined by MICs using bioluminescence rather than traditional turbidity measurement, using sterile 96-well black-sided plates to generate a checkerboard of 2-fold dilution series from columns 1 to 11 (column 12 = zero) for silver and from rows 1 to 7 (row 8 = zero) for chitosan acetate in 50% nutrient broth. A bacterial suspension (10 μl containing 10^4 cells) was added to each well, and the plate was incubated at 37°C for 15 h with vigorous shaking. The bacterial luminescence was monitored with a luminescence plate reader (MicroBeta Trilux 1450; PerkinElmer Life and Analytical Sciences Inc., Wellesley, MA). The experiments were repeated three times.

***In vitro* killing assays.** Cells were grown overnight in BHI at 37°C and regrown in fresh medium for 2 to 3 h before being collected by centrifugation and suspended in deionized water, used because it lacks chloride ions present in phosphate-buffered saline (PBS) that would interfere with silver. A cell suspension consisting of 10^8 cells/ml was incubated with various concentrations of the chitosan acetate and/or nanoparticle silver for 30 min at room temperature in the dark. After incubation, 100-μl aliquots were taken from each sample to determine CFU. The aliquots were serially diluted 10-fold in PBS to give dilutions of 10^{-1} to 10^{-5}, in addition to the original concentration, and 10-μl aliquots of each of the dilutions were streaked horizontally on square BHI plates by the method of Jett and colleagues (29). The plates were streaked in triplicate and incubated for 12 to 18 h at 37°C in the dark to allow colony formation.

Animals. All animal procedures were approved by the Subcommittee on Research Animal Care (IACUC) of Massachusetts General Hospital and met the guidelines of the National Institutes of Health. Adult female BALB/c mice (Charles River, Wilmington, MA), 6 to 8 weeks old and weighing 17 to 21 g, were used in the study. The animals were housed one per cage and maintained on a 12-hour light/dark cycle with access to food and water *ad libitum*.

Creation of burn injuries and bacterial infection. Mice were shaved on the back and depilated with Nair (Carter-Wallace Inc., New York, NY) 1 day before the creation of burns. The next day, the mice were anesthetized with intraperitoneal injections of a ketamine-xylazine cocktail, and burns were created by applying two preheated (~95°C) brass blocks (10 mm by 10 mm; Small Parts, Inc., Miami, FL) to the opposing sides of an elevated skin fold on the dorsal surface of the mouse for 60 s (nonlethal full-thickness third-degree burns). The combined brass block area was 20 mm by 10 mm, giving an area of 200 mm^2, corresponding to 5% of the total body surface area (TBSA). Immediately after the creation of burns, the mice were resuscitated with intraperitoneal injections of 0.5 ml sterile saline (Phoenix Scientific Inc., St. Joseph, MO).

Five minutes after the creation of the burns (allowing the burns to cool down), a suspension (40 μl) of bacteria in sterile PBS containing 10^8 CFU was inoculated onto the surface of each burn with a yellow-tipped pipette and then smeared onto the burn surface with an inoculating loop.

Treatment of burn infection. Silver-chitosan acetate or nonsilver chitosan acetate bandages (HemCon Medical Technologies Inc.) were applied to the infected burns 15 min after the application of bacteria, allowing the bacteria sufficient time to bind to the burned tissue. To allow adherence of the bandages to the burns, both types of bandages were moistened with MilliQ water before application. In contrast to human third-degree burns, mouse third-degree burns have a dry texture, irrespective of whether they have been contaminated or infected with bacteria. It was therefore necessary to regularly moisten the silver-chitosan acetate bandages to allow the active antimicrobial ingredient (Ag ions) to percolate into the burned tissue. In order not to compromise the activity of the nanocrystalline silver from the silver bandages by using buffers, we used pure water to do this. We had previously shown that pH 4.5 acetate buffer used to moisten chitosan acetate does not alone have an antibacterial effect on *P. aeruginosa* in the short term (hours). Therefore, nonsilver chitosan acetate bandages adhering to the burns were moistened daily with 100 μl of 50 mM sodium acetate buffer, and silver bandages were moistened with MilliQ water.

Bioluminescence imaging. The low-light imaging system (Hamamatsu Photonics KK, Bridgewater, NJ) has been previously described. Briefly, it consisted of an intensified charge-coupled device (CCD) camera mounted in a light-tight specimen chamber fitted with a light-emitting diode, a setup that allowed a background gray-scale image of the entire mouse to be captured. In the photon-counting mode, an image of the emitted light from the bacteria was captured using an integration time of 2 min at a maximum setting on the image intensifier control module. By the use of ARGUS software (Hamamatsu Photonics), the luminescence image was presented as a false-color image superimposed on the grayscale reference image. The image-processing component of the software calculated the total pixel values from the luminescence images of the infected wound area. The infection time was defined as the time during which any bioluminescence was present in the wound when measured at the most sensitive setting.

Follow-up. During the experiment, mice underwent bioluminescence imaging immediately after bacteria were added and at 24-h intervals thereafter. The mice were also followed daily for weight and survival. When mice died (or were sacrificed due to their moribund condition), 5 ml sterile saline was injected into the abdominal cavities of the mice and then withdrawn and cultured on BHI agar plates to determine the presence of *P. aeruginosa* in the peritoneum. Blood samples were also taken from the hearts removed from dead mice and streaked on BHI agar plates.

Statistical methods. Drug interaction analysis. The isobolographic drug interaction analysis is based on the Loewe additivity (no-interaction) theory (1), which is described by the equation

$$1 = \frac{\text{cc (Ag)}}{\text{CA (ag)}} + \frac{\text{cc(chit)}}{\text{CA(chit)}} \quad (1)$$

where cc(Ag) and cc(chit) are the concentrations of the nanoparticle silver and

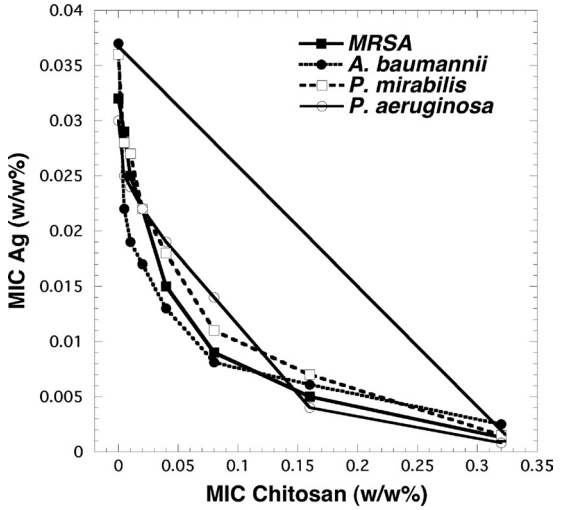

FIG. 1. Isobolographs for MIC studies with single agents and a combination. Checkerboard broth microdilution MIC assays were performed as described in Materials and Methods. The MIC values for nanoparticle silver and for chitosan acetate were plotted against each other for the four species.

chitosan acetate, respectively, in the combination that elicits a certain effect, and CA(Ag) and CA(chit) are the isoeffective concentrations of the nanoparticle silver and chitosan acetate, respectively, acting alone. In isobolographic analysis, the concentration-effect curve of the drugs in combination at a fixed ratio is compared with the theoretical additive concentration-effect curve calculated from equation 1, and the interaction is assessed at any effect level.

An interaction index (I) for each combination ratio was then calculated as [cc(Ag)/CA(Ag)] + [cc(chit)/CA(chit)] for each replicate.

The average of the interaction indices for the three replicates of each strain was calculated. In order to test whether the I values of the three replicates were significantly lower or higher than 1 ($P < 0.05$), the I values were log transformed to approximate a normal distribution, and the 95% confidence intervals were calculated. If the 95% confidence intervals of the I values of a fixed-ratio combination were significantly lower or higher than 1, synergy or antagonism, respectively, was concluded to be present for that particular fixed ratio. The results of isobolographic analysis can be easily visualized using isobolograms. An isobologram is a two-dimensional plot in which the coordinates are the concentrations of the two drugs on an arithmetic scale. An isobol is a curve that starts from a concentration of nanoparticle silver on the *x* axis and ends at an isoeffective concentration of chitosan acetate on the *y* axis, connecting the concentrations of all combinations showing the same effect. An additive isobol, the graphical representation of equation 1, is a straight line from the *x* axis to the *y* axis that connects the isoeffective concentrations of silver and chitosan alone. An isobol that deviates to the left or right from the indifferent isobol indicates synergy or antagonism, respectively.

Statistical comparison of bacterial killing by combinned agents versus killing produced by twice the concentration of each agent acting alone was carried out by 1-way analysis of variance (ANOVA).

All *in vitro* experiments (MIC and killing assays) were repeated three times.

Survival curves were compared by the Kaplan-Meier log-rank test. *P* values of <0.05 were considered statistically significant.

RESULTS

MIC determinations. We determined MIC endpoints by finding the lowest concentration of chitosan acetate and silver that prevented growth, as assessed with a luminescence plate reader. This was necessary because the nanoparticle silver preparation was highly light scattering in nature (more turbid than stationary-phase bacteria), and therefore, traditional turbidometry could not be used.

The MIC values are displayed as classical isobolograms in Fig. 1. From the figure, it can be seen that there was real synergy between the growth-inhibitory effects of chitosan acetate and nanoparticle silver in all the tested bacteria. All the curves were markedly convex to the left of the line, representing additive interaction. The interaction index values are shown in Table 2. The means of these values were significantly less than 1 in all cases ($P < 0.05$). The order of the degrees of synergistic interaction between these four species was as follows: *P. aeruginosa* > *A. baumannii* > *P. mirabilis* > MRSA.

***In vitro* killing assays.** In order to study the possible synergy of the antimicrobial activities of chitosan acetate and silver, killing assays after 30 min of incubation time were performed with Gram-positive bacteria (MRSA) and three different Gram-negative bacteria (*P. mirabilis*, *P. aeruginosa*, and *A. baumannii*) to determine the fraction of viable cells after treatment with chitosan acetate and/or nanoparticle silver preparations. Bacteria were incubated with chitosan acetate and/or nanoparticle silver for 30 min and then plated on BHI agar plates to allow counting of CFU. We used a certain concentration of each material alone that was determined from the MIC graphs and also by experiment and used the combination of silver and chitosan at half of each concentration that was used alone.

Figure 2A shows the antimicrobial activity of chitosan acetate (0.08%) or silver (0.01%) and of a combination (0.04% chitosan plus 0.005% silver) against MRSA. MRSA was the most resistant species tested. There were almost 2 log units of killing with 0.08% chitosan acetate alone and less than 1 log unit of killing with 0.01% silver alone but almost 5 log units of killing with 0.04% chitosan and 0.005% silver ($P < 0.001$ versus either alone).

Figure 2B shows that overall *A. baumannii* was the most susceptible of the four bacterial species. Very low concentrations of both agents were able to produce significant killing. There was almost 1 log unit of killing with 0.0002% chitosan acetate and more than 1 log unit of killing with 0.004% nanoparticle silver but more than 4 log units of killing with the combination of 0.0001% chitosan acetate and 0.002% nanoparticle silver ($P < 0.001$ versus either alone).

Figure 2C shows the killing obtained for chitosan acetate and silver against *P. mirabilis*. There were 1.5 log units of killing with 0.002% chitosan acetate alone and 1.5 log units of

TABLE 2. Interaction indices for combination agents in MIC assays

Chitosan (% [wt/wt])	Interaction index[a]			
	MRSA	*A. baumannii*	*P. mirabilis*	*P. aeruginosa*
0.005	0.697	0.549	0.765	0.415–0.682
0.01	0.673	0.403–0.549	0.765	0.431–0.564
0.02	0.523–0.656	0.329–0.462	0.562	0.329–0.462
0.04	0.380–0.78	0.391–0.525	0.625	0.391
0.08	0.627	0.383–0.517	0.55	0.383–0.516
0.16	1.004	0.633	0.6–0.7	0.566

[a] Interaction indices were calculated using equation 1. For each species, the precise silver concentration used with the specified chitosan concentration shown was the lowest needed to inhibit growth and can be found in Fig. 1. A range is given for triplicate determinations. All values (except that for MRSA at 0.16 chitosan) were significantly less than 1 ($P < 0.05$). Averages (±SD) were as follows: MRSA, 0.75 ± 0.171; *A. baumannii*, 0.591 ± 0.059; *P. mirabilis*, 0.653 ± 0.105; *P. aeruginosa*, 0.478 ± 0.123.

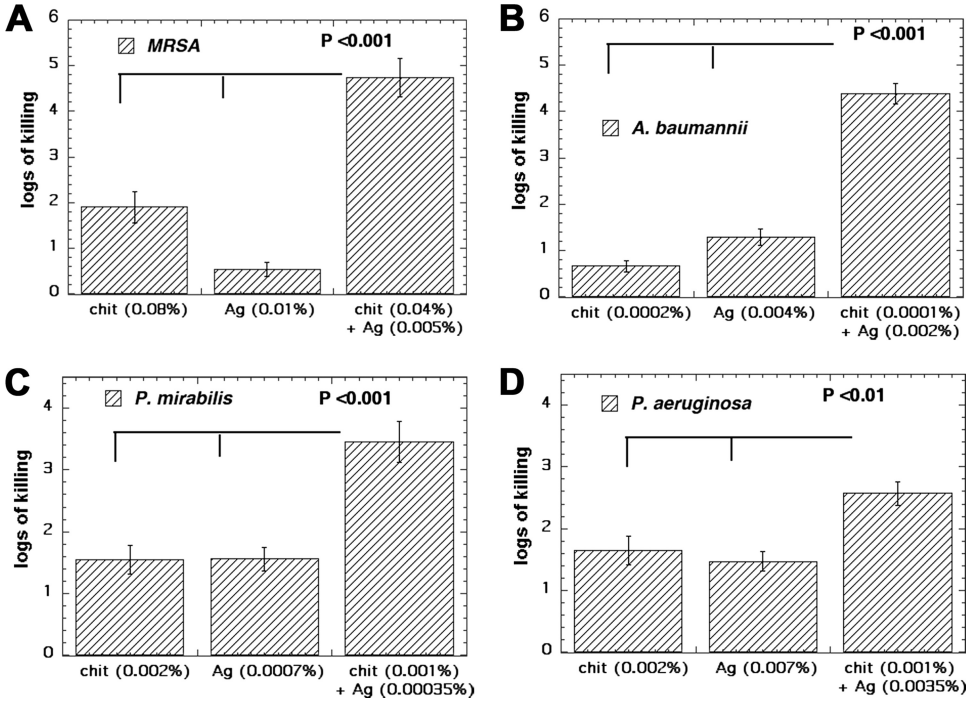

FIG. 2. *In vitro* killing assays with single agents and a combination. Bacteria (10^8/ml) were incubated for 30 min in deionized water with the indicated concentrations of single agents or combinations, followed by serial dilution and plating. (A) MRSA. (B) *A. baumannii.* (C) *P. mirabilis.* (D) *P. aeruginosa.* chit, chitosan.

killing with 0.0007% nanoparticle silver alone but more than 3 log units of killing with the combination of 0.001% chitosan acetate and 0.00035% nanoparticle silver ($P < 0.001$ versus either alone).

Figure 2D shows the killing found for chitosan acetate and silver against *P. aeruginosa*. There were 1.5 log units of killing with 0.002% chitosan acetate and more than 1 log unit of killing with 0.007% nanoparticle silver but 2.5 log units of killing with the combination of 0.001% chitosan acetate and 0.0035% nanoparticle silver ($P < 0.01$ versus either alone).

***In vivo* treatment of infected burns.** Similar to the chitosan acetate bandage, a silver-chitosan acetate bandage adhered extremely well to the surface of the burn when the piece of bandage had been previously moistened with acetate buffer or MilliQ water to render it flexible. The adhesion time of HemCon bandages was >16 days on all surviving mice. We used pieces of both silver-chitosan acetate and nonsilver chitosan acetate that were significantly bigger (>30 mm by 30 mm) (Fig. 3A and B) than the burn itself (~20 mm by 10 mm) (Fig. 3C) because the bacteria sometimes spread laterally into the skin beyond the burned area, as observed by bioluminescence imaging.

Figure 4 shows representative bioluminescence images (collected with the same sensitivity setting on the camera) of mice with *P. aeruginosa*-infected burns treated with silver-chitosan acetate (Fig. 4A) or nonsilver chitosan acetate (Fig. 4B) and with no treatment (Fig. 4C) at day 4 postinfection. Chitosan acetate (nonsilver) was not able to prevent the infection from spreading out of the burned area into the surrounding tissue, although it controlled the infection in the actual area of the burn, while only a small area of infection was observed in the

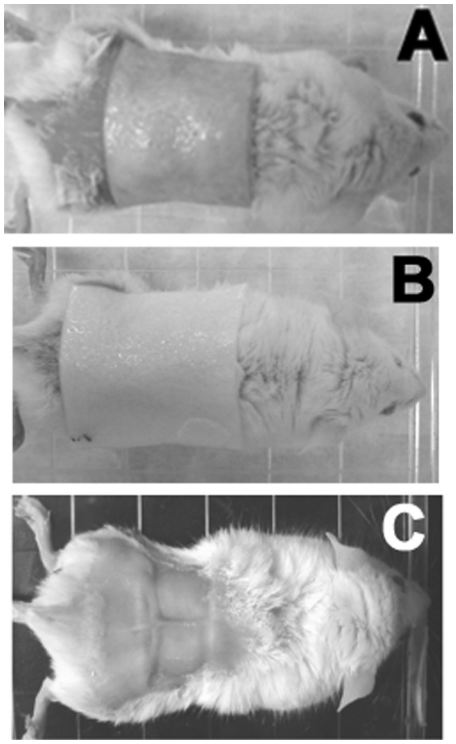

FIG. 3. Representative mice with bandages. (A) Silver-chitosan acetate bandage on burn. (B) Regular (nonsilver) chitosan acetate bandage on burn. (C) No dressing on burn. The squares are the burned areas.

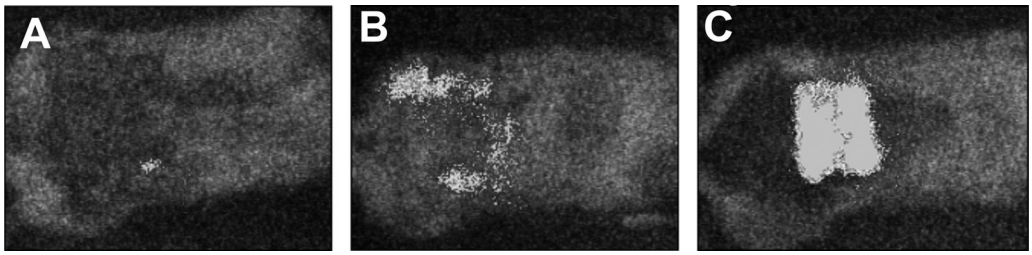

FIG. 4. Representative bioluminescence images. Images (captured at the same bit range of 3) of mice with *P. aeruginosa*-infected burns treated with a silver-chitosan acetate bandage (A) or a regular chitosan acetate bandage (B) or with no treatment (C).

silver-chitosan acetate-treated burn. The untreated burn showed robust bioluminescence signals both in the burn and in the surrounding tissue.

At 3 weeks postinfection, the survival rates of the silver-chitosan acetate-treated group ($n = 14$), the chitosan acetate-treated group ($n = 14$), and the untreated group ($n = 7$) were 64.3%, 21.4%, and 0%, respectively (Fig. 5). The survival curves were found to be significantly different between silver-chitosan acetate-treated and nonsilver chitosan acetate-treated groups ($P = 0.0082$), and between the silver-chitosan acetate-treated group and the untreated group ($P = 0.0055$). No significant difference was found between the survival curves of nonsilver chitosan acetate-treated and untreated groups ($P = 0.68$). In all 3 groups of animals, most of the fatalities (15 out of 20) occurred between 2 and 5 days postinfection.

DISCUSSION

The antibacterial activity of chitosan, arising from its polycationic nature, against a variety of bacteria and fungi is well known (10). We could compare the antimicrobial effects of chitosan acetate against the species in this study. *A. baumannii* was the most susceptible of the tested bacteria. The concentration of chitosan acetate required to completely inhibit *A. baumannii* was 10 times lower than those for other Gram-negative bacteria and 100 times lower than that for the Gram-positive MRSA investigated in this study. Chitosan or its derivatives have been reported to be more effective against Gram-negative bacteria than against Gram-positive bacteria (11). Chung et al. (12) proposed that the negative charge on the cell surfaces of Gram-negative bacteria was higher than that on Gram-positive bacteria. The interaction between the positively charged chitosan and the negatively charged microbial cell wall leads to the leakage of the intracellular constituents. This happens because positively charged nitrogen atoms displace the divalent cations (Ca^{2+} and Mg^{2+}) that help maintain the integrity of the Gram-negative outer membrane by coordinating lipopolysaccharide (LPS). The large size of the chitosan molecule (MW, 460,000) prevents it from entering the bacterial cell, but its cationic character is still able to permeabilize the cells from the outside. The release of divalent cations from the outer membrane triggers the release of LPS and causes the disruption of the permeability barrier of the outer membrane (30).

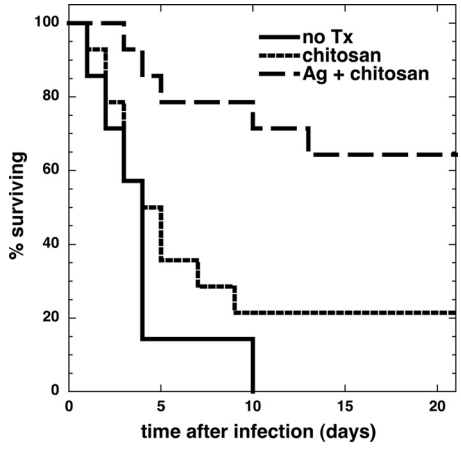

FIG. 5. Survival curves of mice with *P. aeruginosa*-infected burns. *P. aeruginosa*-infected burns were treated with silver HemCon (Ag + chitosan; $n = 14$) or regular HemCon (chitosan; $n = 14$) or received no treatment (no TX; $n = 7$). The survival curves were found to be significantly different between the silver-HemCon-treated group and the regular-HemCon-treated group ($P = 0.0082$) and between the HemCon-treated group and the untreated group ($P = 0.0003$). No significant difference was found between the survival curves of the regular-HemCon-treated and untreated groups ($P = 0.68$).

Silver is well known for its antimicrobial properties and has been used for many years in the medical field for antimicrobial purposes (22). It is used widely in medicine for its distinct antimicrobial action against a broad range of bacteria, yeast, fungi, and viruses (52, 53). Silver exerts its microbicidal effects by interfering with the respiratory chain at the cytochromes (4) or by interfering with components of the microbial electron transport system (21), binding DNA and inhibiting DNA replication (36). Silver in the form of nanoparticles has attracted significant attention (23, 37, 44) in recent years. In the present study, we found that the concentration of nanoparticle silver needed to produce antimicrobial effects was much lower for Gram-negative bacteria than for Gram-positive bacteria. Our results were consistent with those of Rhim et al. (45), who reported Gram-negative bacteria to be more susceptible to the antimicrobial effects of Ag ions than Gram-positive bacteria, presumably due to their thinner cell walls, which may allow more rapid absorption of the ions into the cell (25, 48). Alternatively, silver ions may penetrate more easily through the outer envelope of Gram-negative bacteria than through the outer envelope of Gram-positive bacteria (24).

There have been several publications that have reported various combinations of chitosan and silver to have improved antimicrobial properties. Cao et al. (7) prepared silver-chitosan nanocomposites that inhibited the growth of *S. aureus*

and *Escherichia coli* and proposed these materials as coatings for biomedical-engineering and food-packaging applications (46). Diaz-Visurraga et al. (19) prepared silver-chitosan films that killed *S. aureus*, as shown by electron microscopy, and proposed them for food packaging. Fu et al. (22) prepared multilayer films containing nanosilver and chitosan using an alternative layer-by-layer construction, and these films were effective in killing *E. coli*. They were proposed for coating cardiovascular implants. Kim et al. (31) prepared silver-sulfadiazine-impregnated polyelectrolyte complex sponges composed of chitosan and sodium alginate for wound-dressing applications. The morphological structure of this wound dressing was a dense skin outer layer and a porous cross section layer by scanning electron microscopy. This material had an antimicrobial effect against *P. aeruginosa* and *S. aureus in vitro*. Lu et al. (33) prepared a novel wound dressing composed of nanosilver and chitosan and evaluated its efficacy using wounds in Sprague-Dawley rats, but these wounds were not infected or contaminated by bacteria. Mi et al. (35) prepared a bilayer chitosan membrane using a combined wet/dry phase inversion method that was suitable for topical delivery of silver-sulfadiazine. It displayed activity against *P. aeruginosa* and *S. aureus in vitro* and *in vivo* at an infected wound site. Ong et al. (40) prepared chitosan dressings containing the procoagulant polyphosphate (ChiPP) and silver. Silver-loaded ChiPP exhibited significantly greater bactericidal activity than ChiPP *in vitro* against *P. aeruginosa* and *S. aureus*. The silver ChiPP also significantly reduced mortality from 90% to 14.3% in a *P. aeruginosa* wound infection model in mice. It is difficult to compare the antimicrobial efficacies of different preparations of silver and chitosan, as several variables, such as the precise methods of preparation of both the silver nanoparticles and the chitosan fibers or films, the size of the silver nanoparticles, and the molecular weight and degree of deacetylation of the chitosan, can all be important. To our knowledge, none of these papers demonstrated synergy between chitosan and silver, and the only papers to show effectiveness against an infected wound in mice did not do any comparisons with silver alone or chitosan alone.

The mechanism of action of silver requires that the silver ions enter the bacterial cell for efficient killing. As described above, an important antibacterial mechanism of chitosan is the enhancement of permeability, so it appears entirely reasonable that the interaction of chitosan and nanoparticle silver should be synergistic rather than simply additive. The highest degree of synergy was found with the two Gram-negative species *P. aeruginosa* and *A. baumannii*, consistent with these bacteria being considered to have a high intrinsic permeability barrier. The Gram-negative *P. mirabilis* had an intermediate degree of synergy due to its lower response to permeabilizing agents. The degree of synergy was lowest (although still significant) with Gram-positive MRSA, consistent with the absence of outer membrane permeability barriers in Gram-positive bacteria.

Silver-based medical products, ranging from topical ointments and bandages for wound healing to coated stents, have been proven to be effective in retarding and preventing bacterial infections (9). In our study, we found silver-chitosan acetate-treated mice had a higher survival rate than nonsilver chitosan acetate-treated groups and untreated groups. This was due to the extra antibacterial activity given to the chitosan acetate bandage by the addition of nanoparticle silver.

In conclusion, we have shown that chitosan acetate combined with nanoparticle silver has a significantly synergetic effect on these species, and silver-chitosan acetate on bandages could treat *P. aeruginosa* burn infection in mice, so silver-chitosan acetate bandages could be a promising topical antimicrobial dressing.

ACKNOWLEDGMENTS

This work was funded by a contract from the U.S. Army (W81XWH-08-2-0120) with HemCon Inc., by the U.S. NIH (grants R01A1050875 to M.R.H. and R01CA137108 to Long Y. Chiang), and by the U.S. Air Force MFEL Program (FA9550-04-1-0079). T.D. was supported by Airlift Research Foundation grant 109421.

We are grateful to Xenogen Corp. (Alameda, CA) for the generous gift of bioluminescent bacteria.

M.R.H.'s laboratory has received sponsored research support from HemCon Inc.

REFERENCES

1. **Berenbaum, M. C.** 1989. What is synergy? Pharmacol. Rev. **41:**93–141.
2. **Bjarnsholt, T., et al.** 2008. Why chronic wounds will not heal: a novel hypothesis. Wound Repair Regen. **16:**2–10.
3. **Bjarnsholt, T., et al.** 2007. Silver against Pseudomonas aeruginosa biofilms. APMIS **115:**921–928.
4. **Bragg, P. D., and D. J. Rainnie.** 1974. The effect of silver ions on the respiratory chain of Escherichia coli. Can. J. Microbiol. **20:**883–889.
5. **Burkatovskaya, M., A. P. Castano, T. N. Demidova-Rice, G. P. Tegos, and M. R. Hamblin.** 2008. Effect of chitosan acetate bandage on wound healing in infected and noninfected wounds in mice. Wound Repair Regen. **16:**425–431.
6. **Burkatovskaya, M., G. P. Tegos, E. Swietlik, T. N. P. C. A. Demidova, and M. R. Hamblin.** 2006. Use of chitosan bandage to prevent fatal infections developing from highly contaminated wounds in mice. Biomaterials **27:**4157–4164.
7. **Cao, X. L., C. Cheng, Y. L. Ma, and C. S. Zhao.** 2010. Preparation of silver nanoparticles with antimicrobial activities and the researches of their biocompatibilities. J. Mater. Sci. Mater. Med. **21:**2861–2868.
8. **Caruso, D. M., K. N. Foster, M. H. Hermans, and C. Rick.** 2004. Aquacel Ag in the management of partial-thickness burns: results of a clinical trial. J. Burn Care Rehabil. **25:**89–97.
9. **Chen, J. P.** 2007. Late angiographic stent thrombosis (LAST): the cloud behind the drug-eluting stent silver lining? J. Invasive Cardiol. **19:**395–400.
10. **Chen, S. P., G. Z. Wu, and H. Y. Zeng.** 2005. Preparation of high antimicrobial activity thiourea chitosan-Ag+ complex. Carbohydrate Polymers **60:**33–38.
11. **Chen, Y. M., Y. C. Chung, L. W. Wang, K. T. Chen, and S. Y. Li.** 2002. Antibacterial properties of chitosan in waterborne pathogen. J. Environ. Sci. Health A Tox. Hazard. Subst. Environ. Eng. **37:**1379–1390.
12. **Chung, Y. C., et al.** 2004. Relationship between antibacterial activity of chitosan and surface characteristics of cell wall. Acta Pharmacol. Sin. **25:**932–936.
13. **Church, D., S. Elsayed, O. Reid, B. Winston, and R. Lindsay.** 2006. Burn wound infections. Clin. Microbiol. Rev. **19:**403–434.
14. **Dai, T., et al.** 2010. Topical antimicrobials for burn wound infections. Recent Pat. Antiinfect. Drug Discov. **5:**124–151.
15. **Dai, T., G. P. Tegos, M. Burkatovskaya, A. P. Castano, and M. R. Hamblin.** 2009. Chitosan acetate bandage as a topical antimicrobial dressing for infected burns. Antimicrob. Agents Chemother. **53:**393–400.
16. **Dai, T., et al.** 2009. Photodynamic therapy for Acinetobacter baumannii burn infections in mice. Antimicrob. Agents Chemother. **53:**3929–3934.
17. **Demling, R. H., and L. De Santi.** 2001. Effects of silver on wound management. Wounds **13:**4–9.
18. **Demling, R. H., and M. D. Leslie DeSanti.** 2002. The rate of re-epithelialization across meshed skin grafts is increased with exposure to silver. Burns **28:**264–266.
19. **Diaz-Visurraga, J., A. Garcia, and G. Cardenas.** 2010. Lethal effect of chitosan-Ag (I) films on Staphylococcus aureus as evaluated by electron microscopy. J. Appl. Microbiol. **108:**633–646.
20. **el Kenawy, R., S. D. Worley, and R. Broughton.** 2007. The chemistry and applications of antimicrobial polymers: a state-of-the-art review. Biomacromolecules **8:**1359–1384.
21. **Feng, Q. L., et al.** 2000. A mechanistic study of the antibacterial effect of silver ions on Escherichia coli and Staphylococcus aureus. J. Biomed. Mater. Res. **52:**662–668.

22. **Fu, J., J. Ji, D. Fan, and J. Shen.** 2006. Construction of antibacterial multilayer films containing nanosilver via layer-by-layer assembly of heparin and chitosan-silver ions complex. J. Biomed. Mater. Res. A **79:**665–674.
23. **Furno, F., et al.** 2004. Silver nanoparticles and polymeric medical devices: a new approach to prevention of infection? J. Antimicrob. Chemother. **54:** 1019–1024.
24. **Gogoi, S. K., et al.** 2006. Green fluorescent protein-expressing Escherichia coli as a model system for investigating the antimicrobial activities of silver nanoparticles. Langmuir **22:**9322–9328.
25. **Gray, J. E., et al.** 2003. Biological efficacy of electroless-deposited silver on plasma activated polyurethane. Biomaterials **24:**2759–2765.
26. **Hancock, R. E.** 2007. The end of an era? Nat. Rev. Drug Discov. **6:**28.
27. **Hetrick, E. M., and M. H. Schoenfisch.** 2006. Reducing implant-related infections: active release strategies. Chem. Soc. Rev. **35:**780–789.
28. **James, G. A., et al.** 2008. Biofilms in chronic wounds. Wound Repair Regen. **16:**37–44.
29. **Jett, B. D., K. L. Hatter, M. M. Huycke, and M. S. Gilmore.** 1997. Simplified agar plate method for quantifying viable bacteria. Biotechniques **23:**648–650.
30. **Katsu, T., S. Yoshimura, and Y. Fujita.** 1984. Increases in permeability of Escherichia coli outer membrane induced by polycations. FEBS Lett. **166:** 175–178.
31. **Kim, H. J., et al.** 1999. Polyelectroylte complex composed of chitosan and sodium alginate for wound dressing application. J. Biomater. Sci. Polym. Ed. **10:**543–556.
32. Reference deleted.
33. **Lu, S., W. Gao, and H. Y. Gu.** 2008. Construction, application and biosafety of silver nanocrystalline chitosan wound dressing. Burns **34:**623–628.
34. **MacGowan, J. E. J.** 2001. Year 2000 bugs: the end of the antibiotic era. Proc. R. Coll. Physicians Edinb. **31:**17–27.
35. **Mi, F. L., et al.** 2002. Control of wound infections using a bilayer chitosan wound dressing with sustainable antibiotic delivery. J. Biomed. Mater. Res. **59:**438–449.
36. **Modak, S. M., and C. L. Fox, Jr.** 1973. Binding of silver sulfadiazine to the cellular components of Pseudomonas aeruginosa. Biochem. Pharmacol. **22:** 2391–2404.
37. **Morones, J. R., et al.** 2005. The bactericidal effect of silver nanoparticles. Nanotechnology **16:**2346–2353.
38. **Murray, C. K.** 2007. Infections in burns. J. Trauma **62:**S73.
39. **Nickel, J. C., I. Ruseska, J. B. Wright, and J. W. Costerton.** 1985. Tobramycin resistance of Pseudomonas aeruginosa cells growing as a biofilm on urinary catheter material. Antimicrob. Agents Chemother. **27:**619–624.
40. **Ong, S. Y., J. Wu, S. M. Moochhala, M. H. Tan, and J. Lu.** 2008. Development of a chitosan-based wound dressing with improved hemostatic and antimicrobial properties. Biomaterials **29:**4323–4332.
41. **Paddock, H. N., et al.** 2007. A silver impregnated antimicrobial dressing reduces hospital length of stay for pediatric patients with burns. J. Burn Care Res. **28:**409–411.
42. **Percival, S. L., P. Bowler, and E. J. Woods.** 2008. Assessing the effect of an antimicrobial wound dressing on biofilms. Wound Repair Regen. **16:**52–57.
43. **Rabea, E. I., M. E. Badawy, C. V. Stevens, G. Smagghe, and W. Steurbaut.** 2003. Chitosan as antimicrobial agent: applications and mode of action. Biomacromolecules **4:**1457–1465.
44. **Rai, M., A. Yadav, and A. Gade.** 2009. Silver nanoparticles as a new generation of antimicrobials. Biotechnol. Adv. **27:**76–83.
45. **Rhim, J. W., S. I. Hong, H. M. Park, and P. K. Ng.** 2006. Preparation and characterization of chitosan-based nanocomposite films with antimicrobial activity. J. Agric. Food Chem. **54:**5814–5822.
46. **Sanpui, P., A. Murugadoss, P. V. Prasad, S. S. Ghosh, and A. Chattopadhyay.** 2008. The antibacterial properties of a novel chitosan-Ag-nanoparticle composite. Int. J. Food Microbiol. **124:**142–146.
47. **Schaber, J. A., et al.** 2007. Pseudomonas aeruginosa forms biofilms in acute infection independent of cell-to-cell signaling. Infect. Immun. **75:**3715–3721.
48. **Schierholz, J. M., L. J. Lucas, A. Rump, and G. Pulverer.** 1998. Efficacy of silver-coated medical devices. J. Hosp. Infect. **40:**257–262.
49. **Thomas, V., M. M. Yallapu, B. Sreedhar, and S. K. Bajpai.** 2009. Fabrication, characterization of chitosan/nanosilver film and its potential antibacterial application. J. Biomater. Sci. Polym. Ed. **20:**2129–2144.
50. **Travan, A., et al.** 2009. Non-cytotoxic silver nanoparticle-polysaccharide nanocomposites with antimicrobial activity. Biomacromolecules **10:**1429–1435.
51. **Wei, D., W. Sun, W. Qian, Y. Ye, and X. Ma.** 2009. The synthesis of chitosan-based silver nanoparticles and their antibacterial activity. Carbohydr. Res. **344:**2375–2382.
52. **Wright, J. B., K. Lam, D. Hansen, and R. E. Burrell.** 1999. Efficacy of topical silver against fungal burn wound pathogens. Am. J. Infect. Control **27:**344–350.
53. **Yin, H. Q., R. Langford, and R. E. Burrell.** 1999. Comparative evaluation of the antimicrobial activity of ACTICOAT antimicrobial barrier dressing. J. Burn Care Rehabil. **20:**195–200.